Simulation of Kinematic and Dynamic Models of an Underwater Remotely Operated Vehicle

Viviana Martínez, Daniel Sierra and Rodolfo Villamizar
Escuela de Ingenierías Eléctrica, Electrónica y de Telecomunicaciones
Universidad Industrial de Santander, Bucaramanga, Colombia
Email: blanca.martinez@correo.uis.edu.co
dasierra, rovillam@uis.edu.co

***Abstract*—The implementation of the dynamic and kinematic models of an underwater remotely operated vehicle (VideoRay Pro III) in Matlab/Simulink is presented. The system was built as a closed loop configuration where the inputs are the desired body-fixed velocities or the inertial-frame position and orientation. The block diagram allows for the observation of the UROV states and thrusts exerted by the propellers. The implementation of the VideoRay Pro III models is the initial phase of a research that seeks to establish the instrumentation and computational architecture for the aided inertial navigation of an UROV.**

I. Introduction

An underwater remotely operated vehicle (UROV) is an unmanned robot that communicates with a control station on the sea surface through an umbilical cable used for power and signal transmission [1].

The UROV overall objective is to do a task of some complexity and its capability can be evaluated by its size, operational depth and available working tools [2]. According to this, it is possible to define three categories for this kind of robots: heavy work, observation and mini/micro-ROV [3].

In any of the three categories described, the UROV design introduces research challenges in areas like signal processing, electronic instrumentation and computation. One of the most important tasks is the selection of the sensors and computational architecture that allows for the development of navigation, processing and communication tasks inside the robot, and to facilitate its successful maneuvering.

This paper presents the first advances in a research that seeks an alternative solution to the challenge exposed above. The project proposes to implement an algorithm to estimate the vehicle's position, orientation and velocities from the measurements of linear acceleration and angular rate provided by an inertial measurement unit (IMU). States propagation will be based on the UROV dynamic and kinematic models. During the research development, the inertial sensors will be chosen according to those commercially available, the estimator will be tested, and finally a computational architecture for an UROV will be proposed.

In the initial phase of our work, a simulator for the complete VideoRay Pro III model using Matlab/Simulink was implemented. Through this system the acceleration and angular rate signals needed to test the estimation algorithm were obtained along with the position and orientation to compare the states estimates. The simulator was built taking as reference the ROV Design and Analysis toolbox (RDA) from the Robotic Research Centre at Nanyang Technological University [4]. Likewise, the model parameters were adopted from the work published by Wang and Clark [5].

Fabekovic *et al.* [6] presented in 2007 the implementation of the VideoRay Pro II kinematic model with the possibility of hardware in the loop simulation. However, the publication does not have details about the Matlab implemented configuration. Other researchers as Wang [7], Miskovic *et al.* [8] and Karras *et al.* [9] identified the parameters of VideoRay Pro and they simulated the deduced models, but neither of these publications emphasizes on the implementation process.

Simulators for UROVs are of interest because they provide most accurate description of the system that includes the coupling among the movements in six degrees of freedom (6 DOF) in the time domain. The modeling of dynamic, propulsion system, measurement system and environmental disturbances should be capable of reconstructing the time response of the real system using ordinary differential equations that relate the vehicle's position, orientation and velocities [10].

Micro-ROV VideoRay Pro is gaining popularity due to its agility, easy transportation, deployment and recovery, besides its relative low cost which make them suitable to explore places where it is not possible to have access with other underwater devices [11]. That is why a simulation system that helps researchers in the analysis of this vehicle is provided, for example to scientific community in Colombia where this is still an innovative technology.

In this document the assumptions made in the modeling of VideoRay Pro III are specified and a closed loop block diagram for the simulation of the ROV behaviour and visualization of the vehicle's states and thrusters' forces is presented.

The paper is organized as follows: section II summarizes the theory about underwater vehicle modeling needed for the interpretation of the VideoRay Pro parameters which are presented in section III. Section IV shows the block diagram built together with the results of the simulations, and finally section V has the conclusions obtained in this first phase of work.

II. Underwater Vehicle Modeling

Float structures, vessels and partially or completely submerged vehicles such as UROVs are part of the marine craft category [10]. Their movements are described using two reference frames: inertial frame and body-fixed frame.

Inertial reference frame has its origin in an arbitrary point on the surface of the Earth and consists of three perpendicular axes following the right hand rule: x indicates North, y points to the East, and z points towards the center of the Earth [12]. This frame is considered inertial because the rotation of the Earth does not affect significantly the marine vehicles at low speed [1].

Likewise, the body-fixed frame consists of three axes according to the right hand rule: x goes from stern to bow, y from port to starboard, and z indicates the UROV descent direction or the increasing in depth from the sea surface. Commonly, the vehicle's axes match its principal axes of inertia and the origin of this reference frame is in the center of gravity [12].

In each frame, six degrees of freedom are identified and they correspond to the six independent coordinates needed to define the twelve states of the vehicle: inertial position and orientation, linear velocity and angular rate. These states form the kinematic and dynamic models of an UROV.

A. kinematic model

Linear displacement in the three inertial axes defines the position vector of the vehicle:

$$\boldsymbol{\eta_1} = \begin{bmatrix} x & y & z \end{bmatrix}^T \tag{1}$$

In the same way, the rotations around each axis of the Earth system, represented by the Euler angles, make up the orientation vector:

$$\boldsymbol{\eta_2} = \begin{bmatrix} \phi & \theta & \psi \end{bmatrix}^T \tag{2}$$

The position and orientation change with respect to time defines the linear velocity and angular rate expressed in the body-fixed frame through the vectors ν_1 and ν_2 respectively:

$$\boldsymbol{\nu_1} = \begin{bmatrix} u & v & w \end{bmatrix}^T \tag{3}$$

$$\boldsymbol{\nu_2} = \begin{bmatrix} p & q & r \end{bmatrix}^T \tag{4}$$

Fig. 1 shows the location of the reference frames and their relation with the robot's states. According to the Society of Marine Architects and Naval Engineers (SNAME) [13], the directions of the linear movements are named surge, sway and heave, and the rotational ones roll, pitch, and yaw.

The evolution of the position and orientation of the UROV is described by (5)-(6) [14]:

$$\dot{\boldsymbol{\eta}}_1 = \boldsymbol{J_1}\left(\boldsymbol{\eta_2}\right)\boldsymbol{\nu_1} \tag{5}$$

$$\dot{\boldsymbol{\eta}}_2 = \boldsymbol{J_2}\left(\boldsymbol{\eta_2}\right)\boldsymbol{\nu_2} \tag{6}$$

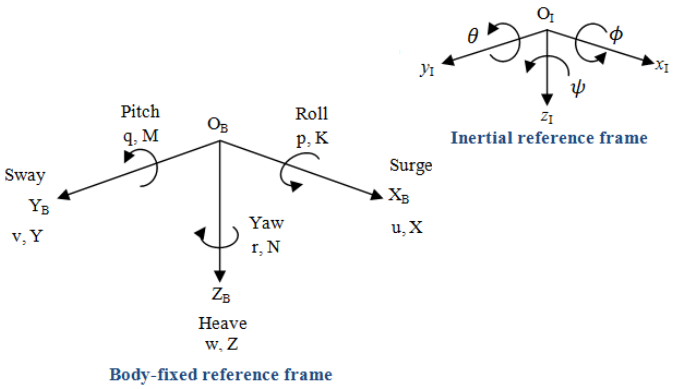

Fig. 1. Reference frames of an UROV. The origin of the inertial frame is at an arbitrary point on the surface of the Earth and the position and orientation are described in it. The origin of the body-fixed frame coincides with its center of gravity and the linear velocities and angular rate are related to it.

where,

$$\boldsymbol{J_1} = \begin{bmatrix} c\theta c\psi & (-c\phi s\psi + s\phi s\theta c\psi) & (s\phi s\psi + c\phi s\theta c\psi) \\ c\theta s\psi & (c\phi c\psi + s\phi s\theta s\psi) & (-s\phi c\psi + c\phi s\theta s\psi) \\ -s\theta & c\theta s\psi & c\theta c\phi \end{bmatrix} \tag{7}$$

$$\boldsymbol{J_2} = \left(\frac{1}{c\theta}\right)\begin{bmatrix} c\theta & s\phi s\theta & c\phi s\theta \\ 0 & c\phi c\theta & -s\phi c\theta \\ 0 & s\phi & c\phi \end{bmatrix} \tag{8}$$

Equations (1)-(8) (c: cosine, s: sine) can be described in the matrix form of (9)-(12) and they are used to determine the inertial movements of the robot from its linear velocities and angular rates without regard on the forces and moments that cause them. Nevertheless, to simulate these velocities, it is necessary to know the dynamics of the UROV.

$$\dot{\boldsymbol{\eta}} = \boldsymbol{J}\left(\boldsymbol{\eta}\right)\boldsymbol{\nu} \tag{9}$$

$$\boldsymbol{\eta} = \begin{bmatrix} \boldsymbol{\eta_1} \\ \boldsymbol{\eta_2} \end{bmatrix} \tag{10}$$

$$\boldsymbol{\nu} = \begin{bmatrix} \boldsymbol{\nu_1} \\ \boldsymbol{\nu_2} \end{bmatrix} \tag{11}$$

$$\boldsymbol{J}\left(\boldsymbol{\eta}\right) = \begin{bmatrix} \boldsymbol{J_1}\left(\boldsymbol{\eta_2}\right) & \boldsymbol{0_{3x3}} \\ \boldsymbol{0_{3x3}} & \boldsymbol{J_2}\left(\boldsymbol{\eta_2}\right) \end{bmatrix} \tag{12}$$

B. Dynamic model

When a rigid body is maneuvered in water, it is necessary to take into account the forces and moments caused by the presence of the fluid. They are grouped under the name of generalized hydrodynamic forces and are classified as [15]:

- Radiation-induced forces: they are caused by the fluid inertia surrounding the ROV and generate an added mass and hydrodynamic damping.
- Restoring forces: they are originated due to the gravity and buoyancy forces acting on the vehicle.

- Environmental disturbances: they include the ocean currents, wind and waves generated by wind. However, after certain depth, the UROVs are influenced only by the ocean current.

Including the hydrodynamic forces on the equation of movement of a rigid body [16]:

$$\boldsymbol{M\dot{\nu}} + \boldsymbol{C}(\boldsymbol{\nu})\boldsymbol{\nu} + \boldsymbol{D}(\boldsymbol{\nu})\boldsymbol{\nu} + \boldsymbol{g}(\boldsymbol{\eta}) = \boldsymbol{\tau_c} + \boldsymbol{\tau_{prop}} + \boldsymbol{\tau_{cable}} \tag{13}$$

where,
$\mathbf{M}$ is the total mass matrix;
$\boldsymbol{C}(\boldsymbol{\nu})$ is the centripetal and Coriolis forces matrix;
$\boldsymbol{D}(\boldsymbol{\nu})$ is the hydrodynamic damping matrix;
$\boldsymbol{g}(\boldsymbol{\eta})$ is the restoring forces vector;
$\boldsymbol{\tau_c}$ is the environmental disturbances vector;
$\boldsymbol{\tau_{prop}}$ is the resultant forces and moments vector: $\begin{bmatrix} X & Y & Z & K & M & N \end{bmatrix}$, and,
$\boldsymbol{\tau_{cable}}$ is the cable disturbances vector.

Both the structure and the components of each matrix and vector depend on the design of the UROV and its physical parameters which can be obtained either by fluid mechanics theory or using experimental techniques [12].

III. VideoRay Pro Modeling

The VideoRay Pro is a mini-ROV (or mini-UROV) manufactured by VideoRay[1] that has been used by researchers around the world to develop and test control strategies [7], parameter estimation algorithms [9], and modules to transform an UROV in an autonomous underwater vehicle (AUV) [17], among others.

The modeling of this section is based on the results published by Wang and Clark [5], who made the identification of the physical, mechanical and hydrodynamic parameters of VideoRay Pro III. This UROV is symmetrical with respect to the *x-z* plane, approximately symmetrical with respect to the *y-z* plane and the symmetry with respect to the final plane is assumed because the vehicle moves at low speed.

The above assumptions allow for some simplifications on (13). The matrices that are part of the final model are presented here.

A. Total mass matrix

The UROV total mass corresponds to the mass and inertia of this rigid body along with the added mass due to the radiation-induced forces. It is represented by the diagonal matrix of (14), where m is the true mass of the VideoRay Pro III, I_{xx}, I_{yy}, and I_{zz} are the diagonal components of the UROV inertia tensor, and $X_{\dot{u}}$, $Y_{\dot{v}}$, $Z_{\dot{w}}$, $K_{\dot{p}}$, $M_{\dot{q}}$, and $N_{\dot{r}}$ are the elements that account for added mass and relate the six force/moment components to the six linear/angular accelerations.

$$\begin{aligned}\mathbf{M} = diag(&m - X_{\dot{u}}, m - Y_{\dot{v}}, m - Z_{\dot{w}}, I_{xx} - K_{\dot{p}},\\ &I_{yy} - M_{\dot{q}}, I_{zz} - N_{\dot{r}})\end{aligned} \tag{14}$$

[1] http://videoray.com/

B. Centripetal and Coriolis forces matrix

The fluid inertia surrounding the UROV also causes a contribution to the centripetal and Coriolis forces experimented by the robot. It is described as:

$$\boldsymbol{C}(\boldsymbol{\nu}) = \begin{bmatrix} \mathbf{0_{3x3}} & \boldsymbol{C_{12}}(\boldsymbol{\nu}) \\ -\boldsymbol{C_{12}^T}(\boldsymbol{\nu}) & \boldsymbol{C_{22}}(\boldsymbol{\nu}) \end{bmatrix} \tag{15}$$

$$\boldsymbol{C_{12}}(\boldsymbol{\nu}) = \begin{bmatrix} 0 & mw - Z_{\dot{w}}w & -mv + Y_{\dot{v}}v \\ -mw + Z_{\dot{w}}w & 0 & mu - X_{\dot{u}}u \\ mv - Y_{\dot{v}}v & -mu + X_{\dot{u}}u & 0 \end{bmatrix} \tag{16}$$

$$\boldsymbol{C_{22}}(\boldsymbol{\nu}) = \begin{bmatrix} 0 & I_{zz}r - N_{\dot{r}}r & -I_{yy}q + M_{\dot{q}}q \\ -I_{zz}r + N_{\dot{r}}r & 0 & I_{xx}p - K_{\dot{p}}p \\ I_{yy}q - M_{\dot{q}}q & -I_{xx}p + K_{\dot{p}}p & 0 \end{bmatrix} \tag{17}$$

C. Hydrodynamic damping matrix

Hydrodynamic damping in UROVs is caused mainly by the fluid viscosity that generates lift and drag forces. These are grouped in a diagonal matrix of linear and quadratic terms:

$$\begin{aligned}\boldsymbol{D(\nu)} = diag(&X_u + X_{u|u|}|u|, Y_v + Y_{v|v|}|v|, Z_w + Z_{w|w|}|w|,\\ &K_p + K_{p|p|}|p|, M_q + M_{q|q|}|q|, N_r + N_{r|r|}|r|)\end{aligned} \tag{18}$$

D. Restoring forces vector

When a rigid body is submerged in a fluid, the effect of gravity and buoyancy has to be taken into account. The combination of these effects results in the vector of (19), where W is the weight of the UROV and B its buoyancy.

$$\boldsymbol{g}(\boldsymbol{\eta}) = \begin{bmatrix} (W-B)c\theta \\ -(W-B)c\theta c\phi \\ -(W-B)c\theta s\phi \\ 0 \\ 0 \\ 0 \end{bmatrix} \tag{19}$$

The last components in (19) are zero because we assume that VideoRay Pro III center of gravity is coincident with its center of buoyancy [8].

E. Resultant forces and moments

The vector of resultant forces and moments is obtained through (20). $\boldsymbol{T} \in \Re^{6\times3}$ is the thruster configuration matrix whose components depend on the thrust needed to initiate the movement in the controllable degrees of freedom, and the orientation of the each thruster relative to the UROV center of gravity. $\boldsymbol{C^+}$ and $\boldsymbol{C^-} \in \Re^{3\times3}$ are the diagonal matrices containing the information about the thrusters and $\boldsymbol{u} \in \Re^3$ is the vector of squared angular rates of each propeller, $n_i|n_i|$; $i = 1, 2, 3$. In equation (21), $\frac{d}{2}$ represents the distance from the UROV center of gravity to the center of each horizontal thruster.

$$\boldsymbol{\tau_{prop}} = \begin{cases} \boldsymbol{TC^{+}u} & if \quad n > 0, \\ \boldsymbol{TC^{-}u} & if \quad n < 0. \end{cases} \tag{20}$$

$$\mathbf{T} = \begin{bmatrix} 1 & 1 & 0 \\ 0 & 0 & 0 \\ 0 & 0 & 1 \\ 0 & 0 & 0 \\ 0 & 0 & 0 \\ \frac{d}{2} & -\frac{d}{2} & 0 \end{bmatrix} \tag{21}$$

IV. Implementation at Simulation Level and Results

To simulate the behaviour of the VideoRay Pro III, Matlab/Simulink was used taking as reference the ROV Design and Analysis toolbox (RDA) [4] developed by the Robotic Research Centre at Nanyang Technological University, which is available at Matlab Central[2].

The block diagram for the simulation was built taking into account two scenarios: The first one is a closed loop whose input corresponds to the vector of (11) with the desired velocity components expressed in the body-fixed reference frame, and the outputs are the velocity experimented by the UROV and its linear accelerations in body-fixed frame, and position and orientation relative to the inertial frame.

The second scenario represents a closed loop in which the input is the vector of (10) with the desired position and orientation components in the inertial frame, and the outputs are the same as in the previous case.

In both implemented loops, the error signals corresponding to each degree of freedom are utilized to calculate a vector of control forces and moments based on a PID configuration. This controller is not tuned because it is not fundamental that the states of the ROV follow the reference. A strategy to accomplish the tuning process of a heading controller for VideoRay Pro is presented in [18].

In control theory, it is of interest to find out the variable $\boldsymbol{u}$ or the propeller speed n_i from the control forces and moments [16]. This explains why the blocks that transform this vector in $\boldsymbol{\tau_{prop}}$ through (23) and (20) were included in the model. Also, in the implementation the thrusters saturate when $\boldsymbol{u}$ is out of the range ± 150 according to [5], [7] was taken into account.

$$\boldsymbol{u = C^{-1}T^{-1}\tau_{ctrl}} \tag{22}$$

Fig. 2 shows the diagram that was built to simulate the states of the VideoRay Pro III with a velocity input. The gray blocks in the bottom part of the system are the functions to visualize the outputs of the models, except the block "Load VideoRay Pro III parameters" that, as it name states, loads a *.mat* file containing the needed parameters values to perform the simulation.

[2]http://www.mathworks.com/matlabcentral/fileexchange/19362-rov-design-and-analysis-rda-simulink

A. Velocity reference

The sway, roll and pitch velocities were adjusted to zero because the UROV is not controllable in these degrees of freedom and therefore no velocity in these directions was required. Fig. 3 and Fig. 4 present the linear acceleration and angular rate components experimented by the VideoRay Pro III when a reference surge velocity of $1.286\ m/s$ is placed. As expected, $\dot{u}$ has a significant change in its value. Although there is variation in $\dot{v}$ and r, these changes are in the order of $10^{-8}\ m/s^2$ and $10^{-7}\ rad/s$ so they can be neglected.

B. Position and orientation reference

In this case, the feedback loop was modified to perform the comparison between the real location of the VideoRay Pro III and that established as the reference. Fig. 5 presents the inertial variables when the maximum depth that the UROV can achieve, corresponding to $152\ m$, was placed. According to the results, the vehicle moves in the desired direction and this displacement does not affect the other degrees of freedom.

C. Comparison test

In order to verify if the implemented system can simulate the states of the VideoRay Pro III adequately, a final simulation test was performed imitating the conditions applied for Wang and Clark [5] to the their model.

The loop was opened to directly apply an $\boldsymbol{u}$ signal with $n = 60$ in each horizontal thruster. The results are shown in Fig. 6. As it can be observed, the UROV reaches a constant surge velocity of $0.36\ m/s$. It is $0.11\ m/s$ lower than the $0.47\ m/s$ obtained by Wang and Clark in a surge test performed in a pool, and $0.15\ m/s$ lower than the speed of $0.51\ m/s$ predicted with their simulation.

V. Conclusion

A simulation of dynamic and kinematic models of the VideoRay Pro III using Matlab/Simulink was implemented. Two closed loop diagrams were constructed to simulate the ROV states along with the forces generated by the thrusters and linear accelerations experienced by the vehicle. With one of the loops the inputs correspond to the desired velocities in the body-fixed frame, and in the other one the reference is the inertial position and orientation. Through manipulation of the inputs, we verified that the UROV moves in the indicated direction causing a time evolution of the inertial variables observed.

With the simulator developed, the linear acceleration and angular rate components of the UROV are obtained and can be used as estimator observations. Furthermore, the resulting forces and moments will be used as input for a fusion algorithm for the propagation of the vehicle's states using the complete model of the UROV.

The implementation of models contributes to the analysis of the behaviour of marine vehicles without actual testing involving human resources, equipment and costs. However, it is important to clarify the methodology used for the simulation to allow researchers the adequacy of systems for other robots.

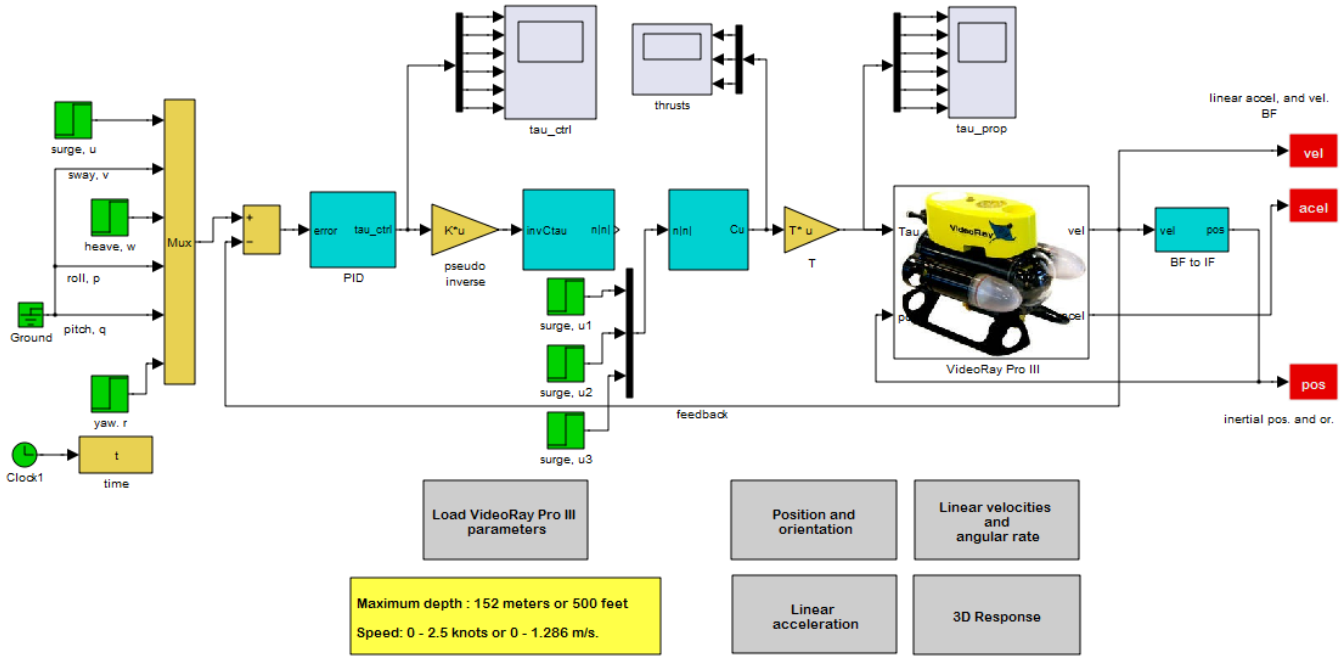

Fig. 2. Simulator for micro-ROV VideoRay Pro III. The inputs are the desired velocities in the body-fixed frame or the required inertial position and orientation, and the outputs are the states of the vehicle.

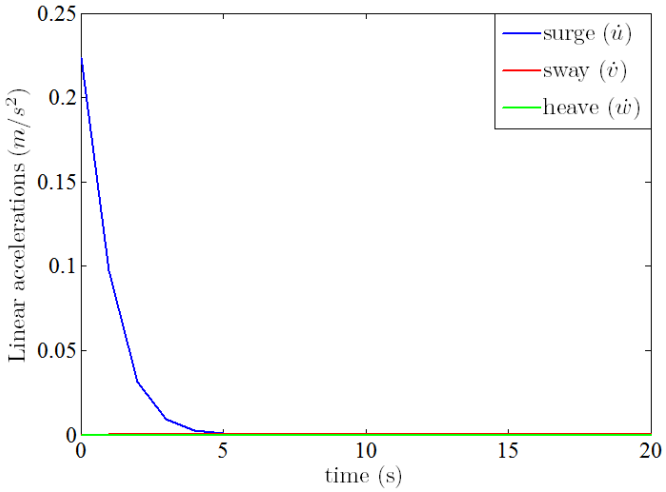

Fig. 3. Linear acceleration experimented by the UROV with a reference input $\nu = [1.286\ 0\ 0\ 0\ 0\ 0]$. There is a significant change in $\dot{u}$ as was expected. There is a very small variation in $\dot{v}$ but it is in the order of 10^{-8} so it can be neglected.

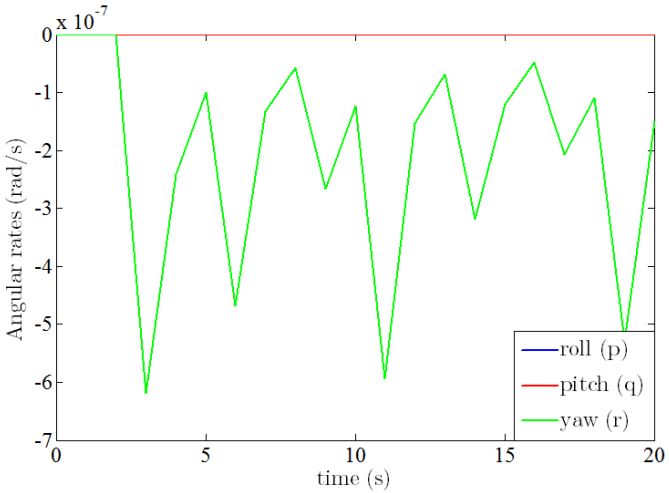

Fig. 4. angular rates experimented by the UROV with a reference input $\nu = [1.286\ 0\ 0\ 0\ 0\ 0]$. The change in r is very small so it can be can be neglected.

The simulator presented in this document does not include environmental perturbations, and forces and moments caused by the umbilical cable. They will be included in a future update to analyze their influence on the evolution of the VideoRay Pro III states.

The tuning of the controller that is part of the loop is another simulation research activity that can be performed using the built system.

References

[1] A. Carlsen, "Navigational assistance for mini-ROV," Master's thesis, Norwegian University of Science and Technology, 2010.

[2] (2012, April) Remotely Operated Vehicles Committee of the Marine Technology Society. [Online]. Available: http://www.rov.org/

[3] L. B. Gutiérrez, J. A. Ramírez, C. A. Zuluaga, R. E. Vásquez, D. A. Flórez, and R. A. Valencia, "Diseo básico de un vehículo operado remotamente (ROV) para inspección subacuática de instalaciones portuarias." in *IEEE Colombian workshop on robotics and automation*, 2007, pp. 1–6.

[4] C. S. Chin, M. W. Lau, E. Low, and G. Seet, "Software for modelling and simulation of a remotely-operated vehicle rov," *International journal of simulation modeling*, vol. 5, no. 3, pp. 114–125, September 2006.

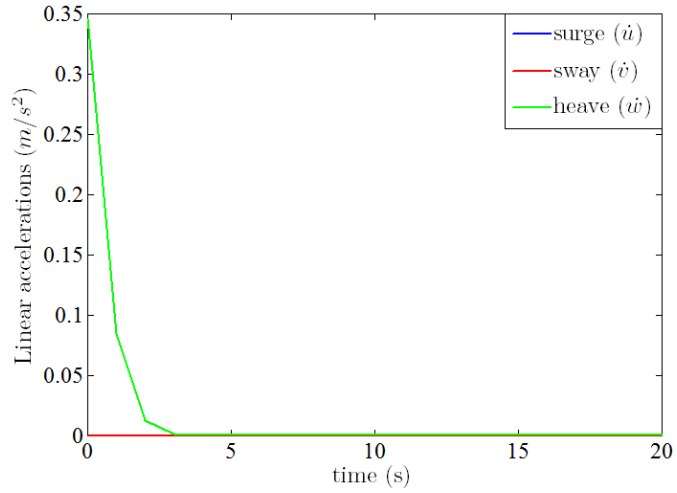

Fig. 5. Linear acceleration experimented by the UROV with a reference input $\eta = [0\ 0\ 152\ 0\ 0\ 0]$. The linear acceleration experimented by the VideoRay Pro III in heave indicates that the vehicle only moves in this direction.

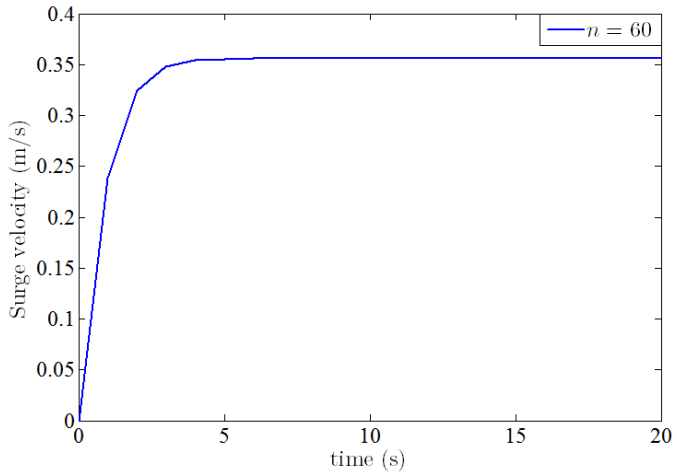

Fig. 6. Surge velocity experimented by the VideoRay Pro III when a constant propeller speed of $n = 60$ is applied to each horizontal thruster.

[5] W. Wang and C. Clark, "Modeling and simulation of the videoray pro III underwater vehicle," in *OCEANS 2006*, 2007, pp. 1–7.

[6] Z. Fabekovic, Z. Eskinja, and Z. Vukic, "Micro rov simulator," in *ELMAR 2007*, 2007, pp. 97–101.

[7] W. Wang, "Autonomous control of a differential thrust micro-ROV," Master's thesis, University of Waterloo, 2006.

[8] N. Miskovic, N. Vukic, and M. Barisic, "Identification of coupled mathematical models for underwater vehicles," in *OCEANS 2007*, 2007, pp. 1–6.

[9] G. Karras, S. Loizou, and K. Kyriakopoulos, "Online state and parameter estimation of an under-actuated underwater vehicle using a modified dual unscented kalman filter," in *IEEE/RSJ International conference on intelligent robots and systems*, 2010, pp. 4868–4873.

[10] T. I. Fossen, *Handbook of marine craft hydrodynamics and motion control*. John Wiley & Sons, 2011.

[11] A. Goldstein and S. Bentley, "Use of highly portable micro-sized remotely operated vehicles for environmental monitoring and mapping," in *OCEANS 2010*, 2010, pp. 1–6.

[12] J. Silva and J. Sousa, *New approaches in automation and robotics*. Intech, 2008, ch. 11, pp. 197–206.

[13] S. of Naval Architects and M. Engineers, "Nomenclature for treating the motion of a submerged body through a fluid," Tech. Rep., 1950.

[14] T. I. Fossen, *Guidance and control of ocean vehicles*. John Wiley & Sons, 1994.

[15] G. Antonelli, T. I. Fossen, and D. Yoerger, *Springer handbook of robotics*. Springer, 2008, ch. 43, pp. 987–1008.

[16] E. Conrado and N. Maruyama, "Intelligent UUV: Some issues on ROV dynamic positioning," *IEEE Transactions on aerospace and electronic systems*, vol. 43, no. 1, pp. 214–226, January 2007.

[17] M. Stipanov, N. Miskovic, Z. Vukic, and M. Barisic, "ROV autonomization-yaw identification and automarine module architecture," in *IFAC World Conference*, 2007, pp. 1–6.

[18] N. Miskovic, Z. Vukic, M. Barisic, and B. Tovornik, "Autotuning autopilots for micro-ROVs," in *14th Mediterranean Conference on Control and Automation*, 2006, pp. 1–6.